Article:
Jia, D, Ngoduy, D and Vu, HL (2019) A multiclass microscopic model for heterogeneous platoon with vehicle-to-vehicle communication. Transportmetrica B: Transport Dynamics, 7 (1). pp. 448-472. ISSN 2168-0566

https://doi.org/10.1080/21680566.2018.1434021

To appear in *XXX*
Vol. 00, No. 00, Month 20XX, 1–28

A multiclass microscopic model for heterogeneous platoon with vehicle-to-vehicle communication

D. Jia[a], D. Ngoduy[b*] and H.L. Vu[c]

[a] *University of Leeds, UK*; [b] *University of Canterbury, New Zealand*; [c] *Monash University, Australia*

(*Received 00 Month 20XX; final version received 00 Month 20XX*)

With the help of inter-vehicle communication (IVC), a group of connected and autonomous (CA) vehicles can drive cooperatively to form a so-called *platoon-based driving pattern*, which has been verified to significantly improve road safety, traffic efficiency and the environmental sustainability. Nevertheless, there is still a long way to go before a full deployment of CA vehicles on roads is viable, which indicates a long lifespan for mixed (heterogeneous) traffic flow consisting of both conventional (human-driven) and CA vehicles. Due to the complicated platoon structure such as the diversity of vehicle dynamics, different information types and the unreliable vehicular communication environment, platoon heterogeneity has become a big challenge for the system modelling and implementation. Specifically, a deep understanding of the dynamics of the heterogeneous platoon is critical to the traffic stability issues for our deployment of the CA vehicles in the near future. This paper aims to develop a unified multiclass microscopic model for a heterogeneous platoon which can explicitly demonstrate the interaction between human-driven and CA vehicles. Two different functions are specified to model the dynamics of both human-driven and CA vehicles, respectively. More specifically, the consensus-based control algorithm is adopted to model the dynamics of CA vehicles and a typical car-following model (such as the intelligent driver model) is used to describe the dynamics of human-driven vehicles. Our proposed integration method allows studying the interplay between these two functions in the heterogeneous platoon. We then theoretically obtain the linear stability condition of the heterogeneous platoon which takes into account the probabilistic delay in the IVC, the penetration of the CA vehicles, and the relative order of the vehicle types in the platoon. Finally, the envisioned model is verified by simulation which couples the vehicular communication and traffic flow dynamics in various scenarios.

Keywords:
Heterogeneous platoon; multiclass microscopic model; vehicle-to-vehicle (V2V) communication; Consensus control; Linear stability

1. Introduction

As a result of the recent fast development in information and communication technologies (ICT), a lot of attentions have been paid into the development of connected traffic systems. Such connected system can be achieved via the vehicle-to-vehicle (V2V) and vehicle-to-infrastructure (V2I) communication which are novel parts of the intelligent transport systems (ITS). In this paper we consider the connected traffic environment to be characterized by the tight coupling between the vehicle's physical dynamics (mobility) and the communication aspects of the vehicle. It has been shown that the deployment of connected and autonomous (CA) vehicles may allow a platoon-based driving pattern,

*Corresponding author. Email: dong.ngoduy@canterbury.ac.nz

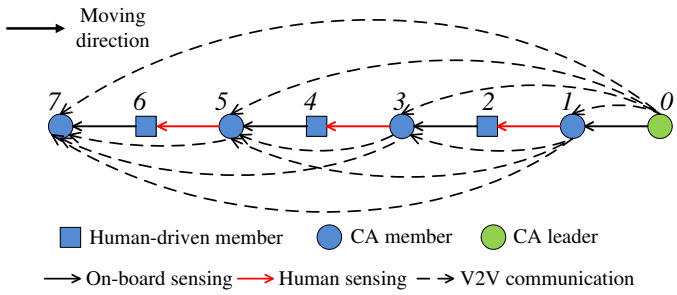

Figure 1. Example of communication topology for a heterogeneous platoon.

and hence can significantly improve road safety, traffic efficiency and the environmental sustainability (van Arem et al. 2006), which, accordingly, has attracted considerable attentions into how to model and control traffic flow dynamics in a connected environment (Dunbar 2012; Öncü et al. 2014; Ge and Orosz 2014; Jia and Ngoduy 2016b,a; Kim et al. 2016; Talebpour and Mahmassani 2016; Ngoduy and Jia 2017; Wang et al. 2016; Gong et al. 2016; Sau et al. 2017).

In the connected traffic flow, with the help of the IVC, CA vehicles in the platoon can timely obtain the information from neighboring vehicles, and then adopt a suitable control law to achieve a certain objective such as maintaining a constant vehicle headway within the same platoon (Jia and Ngoduy 2016a). Control/model schemes for vehicle platooning have been extensively investigated in the recent years (Jia et al. 2016). However, due to the complicated platoon structure such as the diversity of vehicle dynamics, different information types and unreliable vehicular communication environment, the implementation of the homogeneous platooning system is not applicable in practice. In our previous work (Jia and Ngoduy 2016b,a), we characterized the platoon dynamics by an enhanced car-following model which integrates the realistic heterogeneous vehicular communication, wherein the natural limitations and uncertainties in practical vehicular networking such as packet loss and probabilistic transmission delay have been taken into account.

Nevertheless, regarding the modelling of heterogeneous traffic flow, there still exist some issues not fully addressed. Specifically, due to the current limited autonomous technologies and the expensive commercial products, there is still a long way to go before a full deployment of CA vehicles on roads is viable. Consequently, a deep understanding of the dynamics of mixed (heterogeneous) platoon, which consists of both human-driven and CA vehicles, is critical to the deployment of CA vehicles in the near future. This is the main focus of this paper.

Fig. 1 illustrates an example of the communication topology of a heterogeneous platoon with 8 vehicles. First, the interaction between human-driven and CA vehicles is still not well described, which essentially reflects different control models under dynamical communication topologies and is directly related to the traffic stability issue. Most previous work assumed both human-driven and CA vehicles to follow the same control/model function (Kesting et al. 2010a; Ngoduy 2013b,c; Levin and Boyles 2016; Delis et al. 2015), which is not sufficient to precisely characterize the different dynamical interactions between them. In other words, most current models for heterogeneous intelligent traffic flow only assume different parameter sets for human-driven and CA vehicles, hence are conceptually oversimplified to capture the complex dynamics of such heterogeneous intelligent traffic flow as a whole. It is thus more imperative to explore the complex interactions between human-driven and CA vehicles under different functional models describing different driving patterns of human-driven and CA vehicles. Second, it is still not clear how the composition structure of the vehicles including the penetration of CA vehicles as well as their relative positions in the platoon affects the (linear) stability of

traffic flow. For example, a human-driven vehicle can only perceive the kinetic information from its preceding one, as shown in Fig. 1, which may lead to the platoon stability issue.

To tackle these issues, in this paper, we aim to develop a unified multiclass car-following model for a heterogeneous platoon which can explicitly demonstrate the complex interaction between human-driven and CA vehicles. In principle, CA vehicles exhibit many important properties which are different from human-driven vehicle including longitudinal dynamic control (e.g. acceleration/deceleration) and lateral dynamic control (e.g. overtaking, lane-changing,merging/diverging), etc. However, for the proof of concept in this paper, CA vehicles are only referring to longitudinal dynamic control. As such, the CA vehicles in this paper can be considered to include adaptive cruise control or cooperative adaptive cruise control (CACC) vehicles (Kesting et al. 2008, 2010a). To this end, in the proposed model, two different functions are specified to model the dynamics of both human-driven and CA vehicles, respectively. In more details, we extend our previously developed car-following model (Jia and Ngoduy 2016b,a) to capture the dynamics of CA vehicles with the V2V communication capability. Regarding the description of the human-driven vehicle dynamics, we can adopt any typical car-following model such as the optimal velocity model-OVM (Bando et al. 1995), the full velocity difference model-FVDM (Jiang et al. 2001) or the intelligent driver model-IDM (Treiber et al. 2006). It is worth mentioning here that the car-following modeling approach is usually used to describe the observed human behaviour when driving on road such as acceleration/deceleration, lane changing, etc. (Bando et al. 1995; Jiang et al. 2001; Treiber et al. 2006; Kesting et al. 2008, 2010a; Zheng 2014; Saifuzzaman and Zheng 2014; Saifuzzaman et al. 2015).

Our proposed model will tackle the the interaction between human-driven and CA vehicles via the interplay between the two functional forms specified for those human-driven and CA vehicles in a unified expression. From the proposed model structure, our main contributions are to answer the following research questions: What is the (theoretical) stability condition of the heterogeneous platoon where the following factors are all taken into account: 1) the probabilistic packet loss or delay in vehicle-to-vehicle (V2V) communication; 2) the penetration of CA vehicles; and 3) the relative order of the vehicle types in the platoon. Finally, the envisioned model will be verified by simulation which couples the vehicular communication and traffic flow dynamics. In order to do so, we propose a ***bitmap matrix*** to describe the relative position of human-driven/CA vehicle in the platoon, and then integrate it into the proposed multiclass model. Consequently, we provide a unified and explicit expression of the heterogeneous platoon dynamics which includes the platoon composition structure factor. To the best of our knowledge, this is a first attempt that the complex interaction between different functions governing the dynamics of the human-driven and CA vehicles is explicitly demonstrated.

In summary, our main contributions to the state-of-the-art in traffic flow modelling are threefold.

(1) We propose a unified multiclass car-following model for a heterogeneous platoon which theoretically explores the complex interaction between human-driven and CA vehicles.
(2) We theoretically obtain the linear stability condition of the heterogeneous platoon and characterize transient state of heterogeneous platoon, wherein the effects of system parameters such as human perception delays and platoon composition structure are all taken into account.
(3) The model is verified by numerical simulations which couple the traffic dynamics and the vehicular communications. More specifically, the system performance is fully evaluated under various traffic scenarios, for example, to understand how the

penetration of CA vehicles as well as their relative positions in the platoon affect the stability of traffic flow.

The rest of this paper is organized as follows. A brief literature review is given in Section 2. In Section 3, we first generalize a multiclass car-following model for heterogeneous platoons, then we specify the dynamical functions for human-driven and CA vehicles, respectively, and finally formulate these into a consensus problem. In Section 4, we formulate a multiclass car-following model for the heterogeneous platoon, in which the V2V communication delay and platoon composition structure are taken into account. We then investigate the stability of the heterogeneous platoon and explore the impact of heterogeneity of the platoon parameters on the system performance. The simulations are conducted in Section 5 to evaluate the performance of the proposed model, followed by the conclusion in Section 6.

2. Literature review

Some typical control schemes for vehicle platooning have been extensively investigated in the literature, such as the linear control law with the different typical communication topologies (Seiler et al. 2004), the *cooperative adaptive cruise control* (CACC) design (Naus et al. 2010) which adopts the constant time-headway policy with the predecessor-follower information, the sliding-mode control (Fernandes 2012) with the leader-follower information, the influence of information flow topology on the internal stability and scalability of homogeneous vehicular platoons moving in a rigid formation (Zheng et al. 2016). More studies can be found in recent surveys in (Jia et al. 2016; Dey et al. 2016) and references therein.

To address the uncertainties and diversities in the complicated platooning system, the heterogeneous platoon problems have been investigated from different perspectives. In terms of vehicle dynamics, some related work concerns the impact of the heterogeneous parasitic time delays and lags on the longitudinal dynamics of adaptive cruise control (ACC)-equipped vehicles (Ling and Gao 2011), the heterogeneous engine time constant (Ghasemi et al. 2013; Shaw and Hedrick 2007; Lestas and Vinnicombe 2007), etc. In terms of vehicle types, the effect of intelligent vehicles on the multi-class traffic flow dynamics has been extensively considered (Kesting 2007; Kesting et al. 2010a; Ngoduy 2013a,b,c; Kim et al. 2016; Delis et al. 2015; Nikolos et al. 2015). In terms of information types, Xu et al. (2014) quantified the impact of communication information structures and contents on the platoon safety, while Guo and Yue (2011) adopted both global (leader) information via wireless network and local (neighbor) information via on-board sensors. In view of vehicular communication, due to the natural limitations and uncertainties in practical vehicular networking such as transmission range and probabilistic transmission delay, substantial work has been concerning how to design the platooning system under such communication constraints and uncertainties (Qu et al. 2008; Tang et al. 2014; Middleton and Braslavsky 2012; Ghasemi et al. 2013; Monteil et al. 2014; Bernardo et al. 2015; Xu et al. 2014; Jia and Ngoduy 2016b,a). For example, Qu et al. (2008) considered vehicles which are cooperatively driving in case of the dynamically changing communication topologies, Bernardo et al. (2015) considered vehicle platooning in the presence of the time-varying heterogeneous communication delays, and Wang et al. (2014) considered the constant weighted headway spacing control scheme for the heterogeneous platoon to study the influence of time-varying network structures on the platoon dynamics by using a discrete-time Markov chain, etc.

Liu et al. (2017) developed a message dissemination strategy from the vehicular communication perspective, in which a joint control communication design was proposed for

a realistic hybrid traffic flow which is composed of both platoons and individual vehicles. The authors have adopted a consensus-based control mechanism and theoretically analyzed how the stability of the platoon can be affected by various parameters, including message loss due to imperfect inter-vehicle communication. Nevertheless, the dynamics of the mixed traffic platoon have not been considered explicitly in their work.

Notation

For convenience, the notation below will be used for the model development throughout this paper.

Index	
i, j	Vehicle index (increase towards the upstream direction of platoon)
t	Time instant (s)
Traffic dynamic variables	
x_i	Position of vehicle i (m)
v_i	Velocity of vehicle i (m/s)
α_i	Acceleration of V_L, $\bar{\alpha}$ is the maximum (m/s^2)
$\tau^h_{i,i-1}$	Perception delays from human-driven vehicle i to its preceding vehicle $i-1$ (s)
u_i	Control algorithm to minimize state errors
$s_{i,i-1}$	the spacing between vehicle i and its preceding one $(x_{i-1}-x_i)$ (m)
$\Delta v_{i,i-1}$	the speed difference between vehicle i and its preceding one $(v_i - v_{i-1})$ (m/s)
Traffic dynamic parameters	
β, γ	Positive control parameters in control algorithms
V2V Communication parameters	
a_{ij}	Communication link from vehicle j to i
τ^c_{ij}	Beacon dissemination delays from vehicle j to i (s)

3. System modelling

In this section, we first present a generic multiclass car-following model considering the dynamics of both human-driven and CA vehicles, then demonstrate the specifications, assumptions and formulation of the proposed model.

3.1. *Generic multiclass car-following model for heterogeneous connected traffic flow*

The dynamics of an individual vehicle can be described by microscopic (car-following) traffic flow models, which illustrate the acceleration of vehicle i in relation to its leading vehicle $(i-1)$. Traditionally, the acceleration of a vehicle is mainly determined by its velocity, the space headway, and the relative velocity with respect to the leader(s). With the help of the IVC, a vehicle may obtain more information from neighbouring vehicles, which can facilitate the optimal velocity and improve traffic safety and efficiency. As stated previously, any vehicle in the heterogeneous platoon can be described as an agent with four components: 1) vehicle dynamics; 2) information type; 3) communication topology; and 4) control law. It shall be noted that the human-driven vehicle can be regarded as a special CA vehicle with limited connected and autonomous capacities.

Let us now consider vehicles i which drives cooperatively with its neighbours, in which the vehicle may obtain local information from the neighbours via V2V communication (for CA vehicle type) or human perception (in case of the human-driven type). At this

stage of the paper, we ignore the lane-changing process and only consider the traffic dynamics in a single lane roadway so the neighbouring vehicles refer to the (multiple) leading vehicles. Thus the dynamics of vehicle i at time instant t can be determined in a general form:

$$\dot{x}_i(t) = v_i(t) \tag{1}$$

$$\dot{v}_i(t) := u_i(t) = f_i\left(v_i(t), \Gamma_l(s_{i,j}(t), \Delta v_{i,j}(t), ...)\right), j \in \mathcal{N}_i(t) \tag{2}$$

where $x_i \in R$ and $v_i \geq 0$ are the position and velocity of vehicle i, $s_{i,j}(t)$ and $\Delta v_{i,j}(t)$ are the position differences and the velocity differences of vehicle i with respect to its neighbour j, respectively. $\mathcal{N}_i(t)$ denotes the neighbour set of i which can be represented as a directed graph. $\Gamma_l(.)$ describes the corresponding control algorithm for the dynamics of the considered vehicle under the V2V communication. This model can be further extended according to the availability of other type of information, e.g., acceleration. It is worth mentioning that due to the presence of system uncertainties and physical limitations, including *actuator lags* and *sensing delays*, precisely modelling vehicle dynamics is very cumbersome. To simplify the system analysis, in this paper we model the continuous-time dynamics of vehicle i as a *second-order* equation, which has been widely adopted in the literature (see Jia and Ngoduy (2016b,a) and references there-in).

In general, $f_i(.)$ defines a functional form of the car-following rule for vehicle i. For homogeneous traffic flow (i.e.single vehicle class), $f_i(.)$ is identical for all vehicles, that is $f_i(.) \triangleq f(.)$. The specification of $f(.)$ for CA vehicles using a control algorithm for the fully connected traffic system has been described in our previous publications (Jia and Ngoduy 2016b,a), whereas the specification of $f(.)$ for human-driven vehicles follows any current car-following models such as the IDM (Treiber et al. 2006), the OVM (Bando et al. 1995) or the FVDM (Jiang et al. 2001).

In this paper, our objective is to model the heterogeneous platoon which consists of two specific vehicle types: human-driven and CA vehicles. We will first formulate the issue of modeling platoon dynamics into a consensus problem in the rest of this section. Then we will specify two different functional forms $f_i(.)$ for each vehicle class in Section 4, i.e. $f_i(.) = f_{hu}(.)$ for human-driven vehicles and $f_i(.) = f_{ca}(.)$ for CA vehicles, and investigate analytically and numerically how the interplay between $f_{hu}(.)$ and $f_{ca}(.)$ affects the dynamics of the heterogeneous platoon.

3.2. *Communication topology modelling*

The communication topology among platoon members can be generally represented as a directed graph (digraph) $\mathcal{G} = (\mathcal{V}, \mathcal{E}, A)$, where $\mathcal{V} = 1, 2, ..., n$ is the set of vehicles, $\mathcal{E} \subseteq \mathcal{V} \times \mathcal{V}$ is the set of edges, and $A = [a_{ij}] \in \mathrm{R}^{n \times n}$ is an adjacency matrix with nonnegative elements which represents the communication link between vehicle i and j. In this paper, we assume $a_{ij} = 1$ in the presence of a communication link from node j to node i, otherwise $a_{ij} = 0$. In addition, we assume no self-loops in the directed graph, i.e., $a_{ii} = 0$ for all $i = 1, ..., n$. The degree matrices $D = \mathrm{diag}\{d_1, ..., d_n\}$ are diagonal matrices, whose diagonal elements are given by $d_i = \sum_{j=1}^{n} a_{ij}$. The Laplacian matrix of the weighted digraph is defined as $L = D - A$. To study the leader-following problem, we also define a diagonal matrix $B = \mathrm{diag}\{b_1, ..., b_n\} \in \mathrm{R}^{n \times n}$ to be a leader adjacency matrix associated with the system consisting of n vehicles and one leader (labeled with 0), where $b_i = 1$ in presence of a communication link from node i to leader 0, otherwise $b_i = 0$. In case of switching topology (i.e., the communication topology among vehicles

changes due to the packet loss), all adjacency matrices are labeled with the subscript σ.

3.3. *System specifications and assumptions*

In this paper, we specify the core functions of human-driven and CA vehicles in Table 1.

Table 1. Definitions of human-driven and CA vehicles

Component definition	**CA vehicle**	**human-driven vehicle**
Physical dynamics	second-order	second-order
Communication topology	bi-directional communication with front vehicles	only sensing the front vehicle by human perception
Information type	relative position and speed	relative position and speed
Sensing means	on-board sensors	human perception
Control law	fully controlled	human-driven (car-following model)

Specifically, we note that the general concept of *CA vehicle* involves wide capabilities of sensing, communication, control, and even artificial intelligence (Bansal and Kockelman 2017) while in this paper, the CA vehicle is limited to longitudinal movement with V2V communication capability. In addition, unless specified otherwise, we only consider the front vehicles as the neighboring vehicles in this paper, i.e. the forward communication topology is adapted in the envisioned heterogeneous platoon model, which has been verified to provide a quicker response to the traffic perturbations and a better state convergence of a group of vehicles (Jia and Ngoduy 2016a).

The specifications and assumptions for the heterogeneous platooning system are summarized as follows.

(1) The heterogeneous platoon drives on a single lane road, composed of N member vehicles including both CA vehicles and human-driven vehicles, plus a leader vehicle which is labeled with index 0. Note that the vehicle index increases towards the upstream of traffic flow.
(2) Without loss of generality, the platoon leader is assumed a CA vehicle, which is fully controlled externally.
(3) All CA vehicles within the same platoon can connect with each other, which implies that V2V communication range is larger than the platoon length.[1]
(4) The beacon frequency is set to $1/\tau$ (typically 10Hz), and the consensus control is implemented at each end of the control channel interval (CCHI).
(5) For the human-driven vehicles, the perception delay of the preceding vehicle's states is τ^h. The effect of such perception delay on traffic instabilities has been carried out extensively in the literature, for example, by Ngoduy (2015b); Ngoduy and Tampere (2009) and references there-in. For CA vehicles, kinetic states (position and speed) of itself and the preceding one are assumed to be precisely measured by on-board sensors. [2]
(6) The position and velocity function of vehicle are time-continuous, and all vehicles are assumed to maintain a constant speed during each CCHI, i.e., $v_j(t-\tau_j) \approx v_j(t)$, where τ_j is the information communication delay within each CCHI.

It shall be noted that the vehicular communication is dynamic and there are various practical uncertainties in the heterogeneous traffic system, which can be classified by the

[1] under the specification of IEEE 802.11p standard, the typical V2V communication range may reach to 500 meters, which can satisfy practical platoon applications.
[2] To simplify the system analysis, the factor of measured inaccuracies is ignored in the system.

predefined four major components of the system such as the heterogeneous actuator lag, sensing delays, measurement errors, etc. However, since in this paper we mainly focus on the interaction between human-driven and CA vehicles in the heterogeneous platoon, we make some reasonable assumptions on the system modelling to enable the theoretical analysis in the next sections.

According to the function definition in Table 1, any CA vehicle can sense its preceding vehicle's information by on-board sensors. In addition, the CA vehicle can also obtain its neighbors' information via V2V communication in broadcast rather than unicast, which may decrease communication overhead and is feasible in practice. Practically, the driver of a human-driven vehicle can perceive the behaviour of multiple leading vehicles which will lead to a multi-anticipative car-following model to be used for the human-driven vehicles in this paper (see (Ngoduy 2015b) and references there-in). However, for the sake of simplicity, at this stage of the proof of concept the driver of human-driven vehicles is assumed to perceive the only one preceding vehicle's information (i.e. a single anticipation car-following model used). In addition, a human driver is assumed to have the same perception to his preceding vehicle whether it is human-driven or CA. The psychological interaction between human-driven vehicles and autonomous vehicles is an open research question and beyond the scope of this paper.

3.4. *Consensus problem formulation*

In this paper, the expected behaviour of a heterogeneous platoon is to let its members follow the leader's speed asymptotically and maintain a desired space headway among each other. Usually, when the platoon has to move with a reference constant velocity, e.g., v_0, such dynamics can be described as:

$$\dot{x}_0(t) = v_0(t), \quad \dot{v}_0(t) = 0 \tag{3}$$

Normally, the desired space headway is identical for a homogeneous platoon at the given constant velocity. However, for the heterogeneous platoon, the desired space headway varies for different vehicle types. For example, the desired constant space headway between CA vehicle i and its preceding one is normally smaller than that between the human-driven vehicle i and its preceding one which can be calculated according to the human-driven car-following model at the equilibrium state. It shall be noted that in this paper, the desired space headway for human-driven vehicles does not include the impact of the human perception delay. Thus the desired space headway $s^d_{i,0}$ between the platoon leader and member vehicle i is $s^d_{i,0} = \sum_{j=1}^{i} s^d_{j,j-1}$. The consensus of the platoon-based cooperative driving system (CDS) is deemed to be achieved if the state of system Eq. (1)-Eq. (2) satisfies:

For each member $i \in 1, ..., N$,

$$x_i(t) \to x_0(t) - s^d_{i,0}, \quad v_i(t) \to v_0(t) \tag{4}$$

Accordingly, the stability of the heterogeneous platoon from the *consensus perspective* is defined as below:

Definition 1 (Platoon stability)**.** *Given the system Eq. (1)-Eq. (2), if the state of any member i within the same platoon satisfies*

$$\lim_{t->\infty} |x_i(t) - (x_0(t) - s^d_{i,0})| \leq C_p, \lim_{t->\infty} |v_i(t) - v_0(t)| \leq C_v, \tag{5}$$

where C_p and C_v are the constant positive bounded values, then vehicle i is said to reach the (bounded) stability.

To achieve the consensus goal, the continuous-time dynamics control input $u_i \in R$ in Eq. (2) is supposed to be adjusted based on the neighboring information as well as the control function.

4. Multiclass model for heterogeneous platoon with consensus control

4.1. *General control model for CA and human-driven vehicles*

The basic control scheme for any (CA or human-driven) vehicles which are moving in a cooperative platoon pattern is that the vehicle timely calculates the state error between itself and the surrounding vehicles (including the leader) as the control input in order to adjust its desired acceleration. In addition, we choose the forward information topology (i.e. only the preceding vehicles' information is adopted) and the *leader-follower* consensus control algorithm as the car-following rule of the heterogeneous platoon. The general linear control algorithm can be represented by:

$$\dot{v}_i(t) = \sum_{j=1}^{i-1} a_{ij}\{[x_j(t-\tau_{ij}) - x_i(t) - s_{i,j}^d] + \gamma[v_j(t-\tau_{ij}) - v_i(t)]\} \tag{6a}$$

$$+\beta \cdot b_i\{[x_0(t-\tau_{i0}) - x_i(t) - s_{i,0}^d] + \gamma[v_0(t-\tau_{i0}) - v_i(t)]\} \tag{6b}$$

where γ and β are the positive control parameters. τ_{ij} is the time-varying delays that information of vehicle j is received (perceived) by member i within the same platoon. Eq. (6a) represents the vehicle's position and velocity difference between itself and platoon members, respectively, while Eq. (6b) denotes the vehicle's position and velocity difference between itself and the platoon leader. It shall be noted that there are two types of delays in a heterogeneous platoon: communication delay of CA vehicles and perception delay of human-driven vehicles. In principle, the perception delay τ^h caused by driver i can be considered as the equivalent of communication delay τ caused by vehicle $i-1$, i.e. at any time t, the vehicle i can only obtain the information of vehicle $i-1$ at the time of $t-\tau$ in both cases.

It shall be noted that the general control model Eq. (6) is widely adopted in the literature and applicable for both CA vehicles and human-driven vehicles. The information topology expressed by $a_{i,j}$ and b_i is time-varying for CA vehicles but is fixed for human-driven vehicles. Next, we will specify the control model for CA vehicles and human-driven vehicles, respectively. Specifically, four types of car-following combinations in such a typical heterogeneous platoon will be taken into account: CA-following-CA (CC), CA-following-human (CH), human-following-CA (HC) and human-following-human (HH). Note that the effect of different car-follow combinations on (human-driven) heterogeneous traffic flow has been theoretically studied in (Ngoduy 2015a) in which the function governing the vehicle dynamics is identical, i.e. $f_i(.) = f(.) = f_{hu}(.)$. Therefore the linear method in Ngoduy (2015a) is not applicable for the analysis in this paper when the function governing the vehicle dynamics is non-identical, i.e. $f_{hu}(.) \neq f_{ca}(.)$.

4.1.1. Modelling CA vehicles with consensus control

According to the function definition in Table 1, a CA vehicle can obtain its preceding vehicles' information via on-board sensors, whether the preceding vehicle is CA or human-driven. Therefore, car-following combinations of CC and CH are unified in this case. Furthermore, to simplify the analysis, the factor of on-board sensing delay of a CA vehicle can be measured by itself and be equivalent to that of wireless communication delay. Thus the neighbors' information of a CA vehicle is assumed to be obtained via a pure V2V communication.

For CA vehicles, since the communication delays can be accurately recorded, their negative impact can be mitigated by adding a supplement to the vehicle's state estimation. In addition, to deal with the packet loss of the leader's information, we adopt the last available state of the leader to estimate its current state (i.e. $b_i = 1$). Thus, similar to our previous work in (Jia and Ngoduy 2016b,a), the consensus-based car-following rule for CA vehicles is represented by:

$$\begin{aligned}\dot{v}_i^c(t) &= f_i^c\left(v_i(t), s_{i,j}(t), \Delta v_{i,j}(t)\right) \\ &= \sum_{j\in\mathcal{N}_i^c(t)} a_{ij}\{[x_j(t-\tau_j^c) - x_i(t) + v_0(t-\tau_0)\tau_{ij}^c - (s_{i,0}^d - s_{j,0}^d)] + \gamma[v_j(t-\tau_{ij}^c) - v_i(t)]\}\end{aligned} \tag{7a}$$

$$+\beta\{[x_0(t-\tau_0) + v_0(t-\tau_{i0})\tau_0 - x_i(t) - s_{i,0}^d] + \gamma[v_0(t-\tau_{i0}) - v_i(t)]\} \tag{7b}$$

where $\mathcal{N}_i^c(t)$ denotes neighbor set of CA vehicle i under the forward communication topology. The desired acceleration is determined by the state difference (position and velocity) between the vehicle itself and the neighbours:

- (7a) represents the estimated position error between the gap of member i and j at time t with respect to the desired gap $s_{i,0}^d - s_{j,0}^d$. Due to the time delay τ_j of x_j, a common method in the literature is to add the term $v_0(t-\tau_0)\tau_j$ as the desired gap supplement between member i and j, assuming that member j follows the speed of the leader 0 and the velocity error between member i and j.
- (7b) denotes the estimated position error between the gap of member i and leader 0 at time t with respect to the desired gap $s_{i,0}^d$, and the velocity error between member i and leader 0.

Let us define the position and speed errors with respect to the leader as $\bar{x}_i^c \triangleq x_i^c + s_{i,0}^d - x_0$ and $\bar{v}_i^c \triangleq v_i^c - v_0$, substituting Eq. (7) into Eq. (1)-Eq. (2) results in the closed-loop dynamics of the members:

$$\dot{\bar{x}}_i^c(t) = \bar{v}_i^c(t) \tag{8}$$

$$\dot{\bar{v}}_i^c(t) = \sum_{j\in\mathcal{N}_i^c(t)} a_{ij}\{[\bar{x}_j^c(t-\tau_{ij}^c) - \bar{x}_i^c(t)] + \gamma[\bar{v}_j^c(t-\tau_{ij}^c) - \bar{v}_i^c(t)]\} - \beta[\bar{x}_i^c(t) + \gamma\bar{v}_i^c(t)] \tag{9a}$$

$$+\sum_{j\in\mathcal{N}_i^c(t)} a_{ij}\{[v_0(t-\tau_{i0}^c)\tau_{ij}^c-(x_0(t)-x_0(t-\tau_{ij}^c))]+\gamma[v_0(t-\tau_{ij}^c)-v_0(t)]\}$$
$$+\beta\{[v_0(t-\tau_{i0}^c)\tau_{i0}^c-(x_0(t)-x_0(t-\tau_{i0}^c))]+\gamma[v_0(t-\tau_{i0}^c)-v_0(t)]\} \quad (9b)$$

Accordingly, the system can be decoupled into two parts: the neighboring consensus system and the leader's state error system. In case of the constant speed of the leader, $v_0(t-\tau_{ij}^c)=v_0(t-\tau_{i0}^c)=v_0$ and $x_0(t)-x_0(t-\tau_{ij}^c)=v_0\tau_{ij}^c$, the impact of Eq. (9b) is neglected.

Let $\{\tau_1^c,\tau_2^c,...,\tau_m^c\}$, $m\leq N(N-1)/2$ be the enumeration of the delay set $\{\tau_{ij}^c : i,j=1,...N, j<i\}$. Then let the associated edges with the time delay τ_k define a subgraph $\mathcal{G}_k^c$ with corresponding degree matrix D_k^c and adjacency matrix A_k^c. Since to each edge, there is only one delay associated, the subgraph is disjoint, we have $D^c=\sum_{k=1}^m D_k^c$ and $A^c=\sum_{k=1}^m A_k^c$.

Let $\bar{x}^c\triangleq[\bar{x}_1^c,...,\bar{x}_n^c]^T$, $\bar{v}^c\triangleq[\bar{v}_1^c,...,\bar{v}_n^c]^T$, $\bar{\chi}^c\triangleq[\bar{x}^{cT}\bar{v}^{cT}]^T$, and based on Eq. (9), we can obtain the dynamics of the homogeneous platoon with full CA vehicles:

$$\dot{\bar{\chi}}^c(t)=\mathcal{A}_0^c\bar{\chi}^c(t)+\sum_{k=1}^m\mathcal{A}_k^c\bar{\chi}^c(t-\tau_k^c) \quad (10)$$

where

$$\mathcal{A}_0^c=\begin{bmatrix}0_{N\times N} & I_{N\times N}\\ -(D^c+\beta I) & -\gamma(D^c+\beta I)\end{bmatrix},\ \mathcal{A}_k^c=\begin{bmatrix}0_{N\times N} & 0_{N\times N}\\ A_k^c & \gamma A_k^c\end{bmatrix},$$

$$A^c=\begin{bmatrix}0 & & & \\ 1 & 0 & & \\ \vdots & \ddots & \ddots & \\ 1 & \cdots & 1 & 0\end{bmatrix},\ \text{and}\ D^c=\text{diag}\{0,1,...,N-1\}$$

4.1.2. Linear analysis for human-driven vehicles

In a human-driven vehicle the control algorithm is only related to the driver regardless of its preceding vehicle type (i.e. being either CA or human-driven), therefore its dynamics are the same in both HH and HC car-following combinations. Moreover, in such human-driven vehicles the driver can only sense the position difference and the velocity difference with respect to the preceding one. The functional form of $f_{hu}(.)$ for human-driven vehicles with information sensing delays can be represented by:

$$\dot{v}_i^h(t)=f_{hu}\left(v_i(t),s_{i,i-1}(t-\tau_{i(i-1)}^s),\Delta v_{i,i-1}(t-\tau_{i(i-1)}^{\Delta v})\right) \quad (11)$$

where $\Delta v_{i,i-1}(t)=v_i(t)-v_{i-1}(t)$ and, for the sake of simplicity, we can assume that the delay associated with the space headway is as same as the delay associated with the relative speed, that is: $\tau_{i(i-1)}^s=\tau_{i(i-1)}^{\Delta v}=\tau_{i(i-1)}^h$. Note that these delays are caused by the physiological perception of driver i. Model equation Eq. (11) presents a typical (human-driven) car-following model in the literature with time delays. We refer to Ngoduy (2015b) for more details of a generic (human-driven) car-following model with time delays. For the illustration purposes, in the ensuing paper we will adopt the IDM (Treiber et al. 2006)

to describe the dynamics of the human-driven vehicles. Nevertheless, the analytical and numerical results in this paper should hold for any other model types including the OVM (Bando et al. 1995) and the FVDM (Jiang et al. 2001).

To simplify the control model of human-driven vehicles, we linearize the car-following model Eq. (11) taking into account the delays. Consider the equilibrium situation of $f_{hu}(v^e = v_0, s^e = s_{i,i-1}, 0) = 0$, a small position variations $\bar{x}_i^h$ around the equilibrium (i.e. with respect to the leader of platoon) can be expressed by:

$$x_i^h(t) = x_0(t) - s_{i,0} + \bar{x}_i^h(t) \tag{12}$$

$$\dot{x}_i^h(t) = v_i(t) = v_0 + \dot{\bar{x}}_i^h(t) \tag{13}$$

Accordingly, we have:

$$s_{i,i-1}(t - \tau_{i(i-1)}^h) = s_{i,i-1}^e + \bar{x}_{i-1}^h(t - \tau_{i(i-1)}^h) - \bar{x}_i^h(t) + x_0(t - \tau_{i(i-1)}^h) - x_0(t) \tag{14}$$

$$\dot{s}_{i,i-1}(t - \tau_{i(i-1)}^h) = \dot{\bar{x}}_{i-1}^h(t - \tau_{i(i-1)}^h) - \dot{\bar{x}}_i^h(t) = -\Delta v_{i,i-1}(t - \tau_{i(i-1)}^h) \tag{15}$$

Then we have:

(1) for vehicle $i > 1$, the first order Taylor expansion of Eq. (11) leads to:

$$\ddot{\bar{x}}_i^h(t) = f_{hu}^s(\bar{x}_{i-1}^h(t-\tau_{i(i-1)}^h) - \bar{x}_i^h(t)) + f_{hu}^{\Delta v}(\dot{\bar{x}}_i^h(t) - \dot{\bar{x}}_{i-1}^h(t-\tau_{i(i-1)}^h)) + f_{hu}^v \dot{\bar{x}}_i^h(t) + f_{hu}^s(x_0(t-\tau_{i(i-1)}^h) - x_0(t)) \tag{16}$$

where the partial derivatives f_{hu}^v, f_{hu}^s and $f_{hu}^{\Delta v}$ are evaluated at the equilibrium solutions $(v^e, s^e, 0)$.

(2) for vehicle $i = 1$, its dynamics are presented by:

$$\ddot{\bar{x}}_1^h(t) = -f_{hu}^s \bar{x}_1^h(t) - (-f_{hu}^{\Delta v} - f_{hu}^v)\dot{\bar{x}}_1^h(t) + f_{hu}^s(x_0(t - \tau_{i(i-1)}^h) - x_0(t)) \tag{17}$$

It shall be noted that for a human-driven vehicle, the perception delay error of the platoon leader's state, i.e. $f_{hu}^s(x_0(t - \tau_{i(i-1)}^h) - x_0(t))$ in Eq. (16) and Eq. (17), cannot be mitigated by adding a supplement to the vehicle's state estimation as in Eq. (9b) for a CA vehicle. In addition, for a rational driving behavior, the partial derivatives should satisfy (see Ngoduy (2015b) and references there-in).

$$f_{hu}^v \leq 0, \quad f_{hu}^s \geq 0, \quad \text{and} \quad f_{hu}^{\Delta v} \leq 0 \tag{18}$$

To follow Section 4.1.1, we can obtain the dynamics of the homogeneous platoon with pure human-driven vehicles based on Eq. (16) and Eq. (17):

$$\dot{\bar{\chi}}^h(t) = \mathcal{A}_0^h \bar{\chi}^h(t) + \sum_{k=1}^{m} \mathcal{A}_k^h \bar{\chi}^h(t - \tau_k^h) + \Delta \tag{19}$$

where

$$\mathcal{A}_0^h = \begin{bmatrix} 0_{N\times N} & I_{N\times N} \\ -f_{hu}^s(D^h + (B^h - D^h)) & f_{hu}^{\Delta v} D^h + f_{hu}^v B^h \end{bmatrix}, \; B^h = I_{N\times N}, \; D^h = \text{diag}\{0, 1, ..., 1\},$$

$$\mathcal{A}_k^h = \begin{bmatrix} 0_{N\times N} & 0_{N\times N} \\ f_{hu}^s A_k^h & -f_{hu}^{\Delta v} A_k^h \end{bmatrix},\ A^h = \begin{bmatrix} 0 & & & \\ 1 & 0 & & \\ & \ddots & \ddots & \\ & & 1 & 0 \end{bmatrix},$$

$$\text{and } \Delta = \begin{bmatrix} 0_{N\times 1} \\ \delta_{N\times 1}(t) \end{bmatrix} = \begin{bmatrix} 0_{N\times 1} \\ f_{hu}^s T_{N\times 1} \end{bmatrix} \cdot v_0,\ T_{N\times 1} = [\tau_{10}^h, ..., \tau_{n(n-1)}^h]^T$$

4.2. *Unified multiclass model for a heterogeneous platoon*

We will propose in this section a method to theoretically analyse the interactions between CA and human-driven vehicles described by Eq. (10) and Eq. (19).

To investigate the dynamics of the heterogeneous platoon containing both CA and human-driven vehicle types, we first define a bitmap matrix $\mathcal{I}_{N\times N}^c$ which identifies the number and the relative position/order of CA vehicles in the platoon, where its entry ι_{ij}^c is determined by:

$$\iota_{ij}^c = \begin{cases} 1 & \text{if it is a CA vehicle} \,\&\, i = j \\ 0 & \text{otherwise} \end{cases} \tag{20}$$

For convenience, let us also denote $\mathcal{J} = \{j_1, j_2, ..., j_K\}, 1 \le j_1 < j_2 ... < j_K \le N$ as the order number set of K human-driven vehicles in the heterogeneous platoon. Obviously, $\forall j \in \mathcal{J},\ \iota_{jj}^c = 0$

We then investigate how $\mathcal{I}_{N\times N}^c$ affects the adjacency matrix A (i.e. communication topology) of the heterogeneous platoon. By observing the example in Fig. 1, we can get a general format of adjacency matrix A as follows.

$$A = \begin{bmatrix} 0 & & & & \\ 1 & 0 & & & \\ * & 1 & 0 & & \\ \vdots & \ddots & \ddots & \ddots & \\ * & \cdots & * & 1 & 0 \end{bmatrix} \tag{21}$$

where $* = 0/1$, which is determined by the relative position of CA vehicles in the platoon. Obviously, for the heterogeneous platoon which consists of human-driven and CA vehicles *without communication capacity*, its adjacency matrix A is the same as A^h of the pure human-driven platoon.

For the heterogeneous platoon, its adjacency matrix A is composed of two parts: human-driven vehicle related adjacency $(I - \mathcal{I}^c)A$ and CA vehicle related adjacency $\mathcal{I}^c A$. Obviously, we have $(I - \mathcal{I}^c)A = (I - \mathcal{I}^c)A^h$. However, $\mathcal{I}^c A \neq \mathcal{I}^c A^c$ in case of human-driven vehicles being ahead of CA vehicles. Actually, $\mathcal{I}^c A$ can be derived by the fully connected communication topology $\mathcal{I}^c A^c$ subtracting the links from a human-driven vehicle to its following CA vehicles described by A^*, then we have

$$A = \mathcal{I}^c A + (I - \mathcal{I}^c)A = \mathcal{I}^c(A^c - A^*) + (I - \mathcal{I}^c)A^h \tag{22}$$

Similarly, we have the following equations for the heterogeneous platoon:

$$D = \mathcal{I}^c(D^c - D^*) + (I - \mathcal{I}^c)D^h,\ L = \mathcal{I}^c(L^c - L^*) + (I - \mathcal{I}^c)L^h,\ A_k = \mathcal{I}^c(A_k^c - A_k^*) + (I - \mathcal{I}^c)A_k^h, \tag{23}$$

Next, we investigate how to calculate A^*. It shall be noted that for a CA vehicle, not all achievable information is supposed to be utilized in the control algorithms. Specifically, we consider three types of forwarding communication topologies based on the adopted kind of information:

Case 1: All forwarding achievable information as the reference (denoted as AFI), the entry of A^* is determined by:

$$a_{ij}^* = \begin{cases} 1 - \iota_{jj}^c & \text{if} \quad j \leq i-2 \\ 0 & \text{otherwise} \end{cases} \tag{24}$$

Case 2: Only the information between the vehicle and its nearest preceding human-driven vehicle as the reference (denoted as PFI). In this case, the heterogeneous platoon can be essentially regarded as a series of adjacent sub-platoons divided by the human-driven vehicles. Accordingly, the entry of A^* is determined by:

$$a_{ij}^* = \begin{cases} 1 & \text{if} \quad i < j_1, j \leq i-2 \\ 1 & \text{if} \quad j_m \leq i \leq j_{m+1}, j < j_m, j \leq i-2, \quad m = 1, ..., K-1 \\ 1 & \text{if} \quad i > j_K, j_K < j \leq i-2 \\ 0 & \text{otherwise} \end{cases} \tag{25}$$

Case 3: case 2 with the additional cooperative communication (denoted as PFIC). Furthermore, with the help of the cooperative broadcast of the first following CA vehicle, the state of sub-platoon leaders (i.e. human-driven vehicles) can also be reachable to other following CA vehicles of the sub-platoon. In this case, the entry of A^* is determined by:

$$a_{ij}^* = \begin{cases} 1 & \text{if} \quad i < j_1, j \leq i-2 \\ 1 & \text{if} \quad j_m \leq i \leq j_{m+1}, j \leq j_m, j \leq i-2, \quad m = 1, ..., K-1 \\ 1 & \text{if} \quad i > j_K, j_K \leq j \leq i-2 \\ 0 & \text{otherwise} \end{cases} \tag{26}$$

We illustrate these three different cases by an example of a heterogeneous platoon with 1 leader and 8 members, in which vehicle 3 and vehicle 7 are human-driven, and others are CA. The corresponding adjacency matrix A for each case are as follows:

$$\textbf{(1).} \begin{bmatrix} 0 & & & & & & & \\ 1 & 0 & & & & & & \\ 0 & 1 & 0 & & & & & \\ 1 & 1 & 1 & 0 & & & & \\ 1 & 1 & 0 & 1 & 0 & & & \\ 1 & 1 & 0 & 1 & 1 & 0 & & \\ 0 & 0 & 0 & 0 & 0 & 1 & 0 & \\ 1 & 1 & 0 & 1 & 1 & 0 & 1 & 0 \end{bmatrix}, \textbf{(2).} \begin{bmatrix} 0 & & & & & & & \\ 1 & 0 & & & & & & \\ 0 & 1 & 0 & & & & & \\ 0 & 0 & 1 & 0 & & & & \\ 0 & 0 & 0 & 1 & 0 & & & \\ 0 & 0 & 0 & 1 & 1 & 0 & & \\ 0 & 0 & 0 & 0 & 0 & 1 & 0 & \\ 0 & 0 & 0 & 0 & 0 & 0 & 1 & 0 \end{bmatrix}, \textbf{(3).} \begin{bmatrix} 0 & & & & & & & \\ 1 & 0 & & & & & & \\ 0 & 1 & 0 & & & & & \\ 0 & 0 & 1 & 0 & & & & \\ 0 & 0 & 1 & 1 & 0 & & & \\ 0 & 0 & 1 & 1 & 1 & 0 & & \\ 0 & 0 & 0 & 0 & 0 & 1 & 0 & \\ 0 & 0 & 0 & 0 & 0 & 0 & 1 & 0 \end{bmatrix}$$

Remark 1. *The interplay between the functional forms governing the dynamics of the CA vehicles and the human-driven vehicles in the heterogeneous platoon is described via*

the structure of adjacency matrix A. It is clear that this structure is decided not only by the CA vehicles' penetration but also the relative order of the vehicle types in the heterogeneous platoon.

Remark 2. *It is well known that the second smallest eigenvalue of the interaction Laplacian graph, the so-called algebraic connectivity of the graph, quantifies the convergence speed of the consensus algorithm, and larger algebraic connectivity can lead to shorter convergence time (i.e. Finite-Time Consensus Problems for Networks of Dynamic Agents). Therefore, the system performance could be potentially improved by adjusting the composition structure of the heterogeneous platoon.*

Similarly, the format of the leader adjacency matrix can be easily obtained: $B = \text{diag}\{1, *, ..., *\}$, where $* = 0/1$ to be determined by the relative position of CA vehicles in the platoon and the adopted forwarding communication topologies.

Accordingly, from the following equation for a heterogeneous platoon (combined Eq. (10) and Eq. (19)):

$$\bar{\chi} = \begin{bmatrix} \mathcal{I}^c & \\ & \mathcal{I}^c \end{bmatrix} \bar{\chi}^c + \begin{bmatrix} (I - \mathcal{I}^c) & \\ & (I - \mathcal{I}^c) \end{bmatrix} \bar{\chi}^h,$$

we can derive the dynamics of the heterogeneous platoon:

$$\dot{\bar{\chi}}(t) = \mathcal{A}_0 \bar{\chi}(t) + \sum_{k=1}^{m} \mathcal{A}_k \bar{\chi}(t - \tau_k) + \Delta \tag{27}$$

where

$$\mathcal{A}_0 = \begin{bmatrix} 0_{N\times N} & I_{N\times N} \\ -(\mathcal{I}^c(D + \beta \cdot B) + (I - \mathcal{I}^c) f^s_{hu}(D + (B - D))) & -(\gamma \mathcal{I}^c(D + \beta \cdot B) - f^{\Delta v}_{hu}(I - \mathcal{I}^c)D - f^v_{hu}(I - \mathcal{I}^c)B) \end{bmatrix}$$

$$\mathcal{A}_k = \begin{bmatrix} 0_{N\times N} & 0_{N\times N} \\ (\mathcal{I}^c + f^s_{hu}(I - \mathcal{I}^c))A_k & (\gamma \mathcal{I}^c - f^{\Delta v}_{hu}(I - \mathcal{I}^c))A_k \end{bmatrix},$$

and

$$\Delta = \begin{bmatrix} 0_{N\times 1} \\ \delta_{N\times 1}(t) \end{bmatrix} = \begin{bmatrix} 0_{N\times 1} \\ f^s_{hu}(I - \mathcal{I}^c)T_{N\times 1} \end{bmatrix} \cdot v_0, \; T_{N\times 1} = [\tau^h_{10}, ..., \tau^h_{n(n-1)}]^T$$

For convenience, we denote $|\bar{\delta}| := f^s_{hu} v_0 \cdot \max\{(I - \mathcal{I}^c)T_{N\times 1}\}$

4.3. *System analysis*

This part derives some theoretical properties (i.e. the linear stability conditions) of the proposed multiclass model above (i.e. Eq. (27)). Using the Leibniz-Newton formula gives:

$$\bar{\chi}(t - \tau_k) = \bar{\chi}(t) - \int_{-\tau_k}^{0} \dot{\bar{\chi}}(t + s)ds = \bar{\chi}(t) - \sum_{i=0}^{m} \mathcal{A}_k \int_{-\tau_k}^{0} \bar{\chi}(t + s - \tau_i)ds - \int_{-\tau_k}^{0} \Delta(t + s)ds$$

where $\tau_0 \equiv 0$. Substituting this equation into Eq. (27), we can obtain

$$\dot{\bar{\chi}}(t) = F\bar{\chi}(t) - \sum_{k=1}^{m}\sum_{i=0}^{m}\mathcal{A}_k\mathcal{A}_i\int_{-\tau_k}^{0}\bar{\chi}(t+s-\tau_i)ds - \sum_{k=1}^{m}\mathcal{A}_k\int_{-\tau_k}^{0}\Delta(t+s)ds + \Delta \quad (28)$$

where

$$F = \sum_{i=0}^{m}\mathcal{A}_i = \begin{bmatrix} 0_{N\times N} & I_{N\times N} \\ -(\mathcal{I}^c H + f_{hu}^s(I-\mathcal{I}^c)(L+(B-D))) & -(\gamma\mathcal{I}^c H + (I-\mathcal{I}^c)(-f_{hu}^{\Delta v}L - f_{hu}^v B)) \end{bmatrix}, H = L+\beta\cdot B$$

Then we have the following Lemma and Theorem for the heterogeneous platoon. Details of the proof are given in A and B of this paper.

Lemma 1. *F is Hurwitz stable for the proposed heterogeneous platoon model.*

Theorem 1. *Consider the dynamics of the heterogeneous platoon Eq. (27), then there exists a constant $\tau_0 > 0$, such that when $0 \le \tau_j \le \tau_0$ (j=1,...,m), the state error between the members and the leader is uniformly ultimately bounded by some constant C_0:*

$$\lim_{t\to\infty}||\bar{\chi}|| \le C_0 \quad (29)$$

with less than a certain exponential convergence rate η. Moreover, C_0 depends on the number of human-driven vehicles and the perception time delays. In case of fully CA vehicles platoon, $\lim_{t\to\infty}\bar{\chi} = 0$. The bounded convergence rate η is determined mainly by the composition structure of the heterogeneous platoon and the equilibrium of the human-driven vehicles.

Remark 3. *Theorem 1 theoretically characterizes the heterogeneous platoon's dynamics under the proposed control/model algorithms. Furthermore, by analyzing Eq. (B5), for a given heterogeneous platoon, we obtain the following findings:*

(1) The system steady-state errors C_0 are only related to the perception delay caused by human-driven vehicles, as well as the number (penetration) of the CA vehicles in the heterogeneous platoon.
(2) The system transient-state performance can be describe by a convergence rate $\eta = \kappa(1-2\psi\tau)$, which is mainly determined by not only the CA vehicles' penetration but also their order/position in the platoon. Furthermore, the convergence rate can be improved by optimizing the algebraic connectivity of F, which is related to the communication topology of A.
(3) For a given heterogeneous platoon driving with forward V2V communication topology, the optimal composition structure is all human-driven vehicles following all CA vehicle in the platoon.

Similarly, our proposed method can be applied to further model the heterogeneous platoon with multi-types of vehicles (e.g. multi-bands cars), which will be left in our future research.

5. Numerical studies

In this section, we conduct some numerical experiments to support our theoretical results in the previous sections and to evaluate the performance of the proposed cooperative

driving strategies.

5.1. *Simulation settings and scenarios*

In this section we use the PLEXE (Segata et al. 2014) simulator, an open source IVC simulation framework which consists of the network simulator OMNeT++/MiXiM and the road traffic simulator SUMO. OMNET++/MiXiM is used to simulate the V2V communication based on the 802.11p standard, while SUMO simulates the vehicle dynamics with the proposed consensus algorithms. Both components are coupled with each other through a standard traffic control interface (TraCI) by exchanging the Transmission Control Protocol (TCP) messages, while OMNeT++/MiXiM is acting as the TraCI client and SUMO is acting as the TraCI server.

More specifically, we will adopt the IDM (Treiber et al. 2006) to govern the dynamics of the human-driven vehicles. According to Treiber et al. (2006), the car-following model can be expressed as follows:

$$\dot{v}_i^h(t) = a\Big[1 - \Big(\frac{v_i(t)}{v_i^0}\Big)^4 - \Big(\frac{s_i^*(t)}{s_i(t)}\Big)^2\Big] \tag{30}$$

$$s_i^*(t) = s_0 + v_i(t)T_0 + \frac{v_i(t)\Delta v_j(t)}{2\sqrt{ab}} \tag{31}$$

where:

- s_i is the bumper-to-bumper (distance) gap to the preceding vehicle
- s_i^* is the desired distance gap to the preceding vehicle
- s_0 is the minimum bumper-to-bumper gap for completely stopped traffic
- T_0 denotes the safe time gap
- v_i^0 is the desired (free-flow) speed
- a is the maximum acceleration
- b is the desired deceleration

In the IDM, the instantaneous acceleration consists of a free acceleration on the road where no other vehicles are ahead $a[1-(v_i(t)/v_i^0)^4]$, and an interaction deceleration with respect to its preceding vehicle $-a(s_i^*(t)/s_i(t))^2$.

The simulation parameters for VANET are based on the IEEE 802.11p standard, as listed in Table 2. The traffic related parameters, including IDM model and consensus control parameters, used in our experiments are summarized in Table 3.

Table 2. 802.11p Parameter Setting

Parameter	**Value**	**Parameter**	**Value**
Channel data rate	6 Mbps	Slot time	13 μs
SIFS	32 μs	AIFS	71 μs
Preamble length	32 μs	Plcp duration	8 μs
Propagation delay	2 μs	CWmin	7
Beacon frequency	0.1 s	Beacon priority	2
Beacon size	200 bytes	Transmission range R	500 m
CCH interval	46 ms	Sync interval	4 ms

Table 3. Traffic Related Parameters

Parameter	Value	Parameter	Value
Vehicle length	5 m	s^c	15 m
Maximum acceleration a	3 m/s^2	s^h	30 m
Maximum deceleration b	6 m/s^2	Stable speed	25 m/s
Maximum velocity v_0	38 m/s	Standstill distance s_0	2 m
Control gains:	β=10	γ=2,	
Perception time	0.3 s	Actuator lag	0.25s
Platoon size	9	Time gap T_0	1s

According to Ngoduy (2013b), the human-driven traffic flow is unstable with time delays if:

$$\frac{1}{2}\left(\frac{f_{hu}^v}{f_{hu}^s}\right)^2 + \frac{f_{hu}^v f_{hu}^{\Delta v}}{f_{hu}^s f_{hu}^s} - \frac{1}{f_{hu}^s} + \frac{f_{hu}^v}{f_{hu}^s}\tau^h < 0 \tag{32}$$

To this end, under the given IDM model parameter settings, it is rather straightforward to show that the distance gap of 32m for human-driven vehicles leads to a linear stable regime. In addition, we set 15m of distance gap for CA vehicles. To fully evaluate the platoon performance, we also consider the situation of human-driven vehicles which belong to the unstable regime. It is also straightforward to show that a safe time gap parameter $T_0 = 0.56$s while other parameters remain unchanged can guarantee all human-driven vehicles with and without perception delay being in an unstable regime.

Two typical traffic scenarios are considered for the system evaluation:

- An initial phase during which all following vehicles launch from predefined positions (2m deviations from the equilibrium for each vehicle) to finally cooperatively drive at the same constant speed 25m/s regulated by the leader (essentially to mimic a sharp perturbation).
- A continuous small perturbation wherein the leader experiences a sinusoidal disturbance in speed, defined by $\delta(t) = Asin(0.2\pi t)$ where A =2.5m/s (to mimic a common traffic disturbance caused by an abnormal driving behavior).

We then explore the system performance in both steady state and transient state in the ensuing sections.

5.2. *Impact of communication topology*

As stated in Section 4.2, in case of any human-driven vehicles being ahead of any CA vehicles (except the CA leader), there will be three types of forward communication topologies adopted in the control algorithm. In this part, we investigate how different communication topologies affect the system performance. To facilitate the performance comparison of different communication topologies in the platooning system, we adopt the same control parameters for different topologies. The studied heterogeneous platoon is composed of nine vehicles of which the $6th$ one is the human-driven vehicle and the rest are the CA vehicles.

Fig. 2 describes the state errors of the last vehicle (i.e. vehicle 8) and the human-driven vehicle (i.e. vehicle 6) with respect to the state of the platoon leader (i.e. vehicle 0). It can be observed in Fig. 2(a) and Fig. 2(b) that the state errors between the leader and the CA vehicle 8 converge to zero for all the three communication topologies, whilst there remain position errors in the human-driven vehicle 6, as shown in Fig. 2(c). This is because the introduced perception delay by the human-driven vehicle 6 cannot be mitigated in the

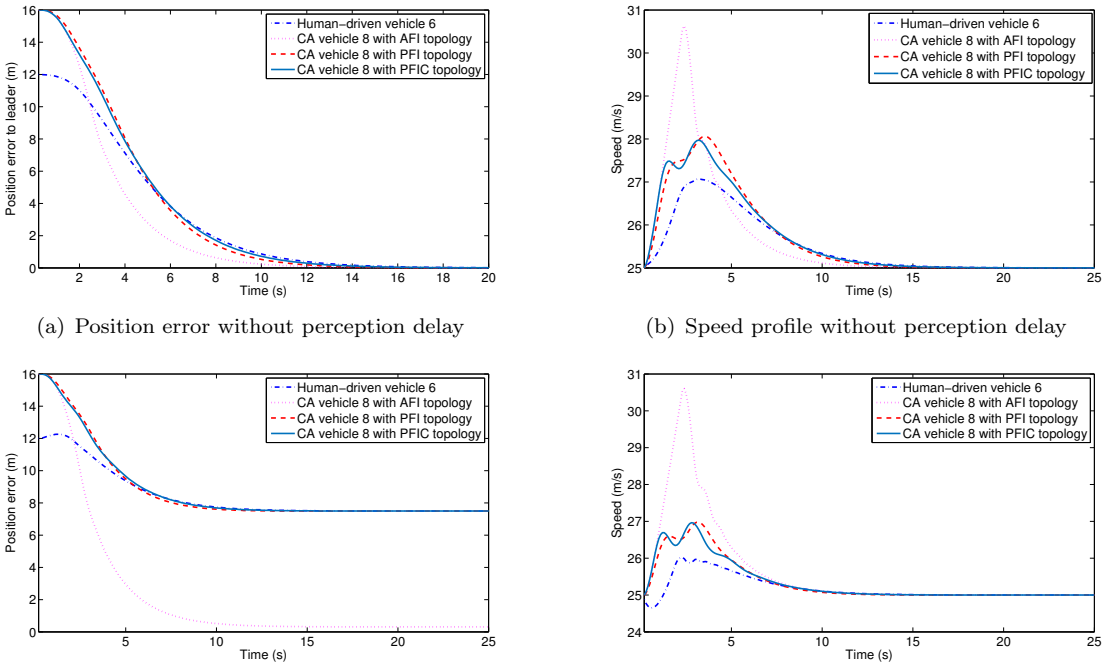

(a) Position error without perception delay

(b) Speed profile without perception delay

(c) Position error with perception delay

(d) Speed profile with perception delay

Figure 2. Heterogeneous platoon dynamics at the initial stage with different forward topologies

proposed control algorithm. Especially, the AFI topology facilitates the position error mitigation (i.e smaller state errors, which are approximately 0 in the stable state), this is due to the leader's information being adopted in the control algorithm. In case of both PFI and PFIC topologies, only information behind the human-driven vehicle 6 is selected as the reference in the control algorithm, which finally leads to the same position error as that of the human-driven vehicle 6 in the stable state. Moreover, among the three types of communication topologies, the AFI topology facilitates the fastest dissipation of the state errors during the initial phase, then followed by the PFIC and the PFI, respectively. This is because the AFI topology provides the most communication links from the preceding vehicles, which fastens the vehicle's response to the leader's behaviour.

However, in case of a human-driven vehicle followed by a CA vehicle, since the CA vehicle is unaware of the perception delay of the human-driven vehicle, the CA vehicle with the AFI topology (i.e. obtaining all of its preceding CA vehicles' information as the reference in the control algorithm) may potentially bring in a safety issue, even lead to a collision with its preceding human-driven vehicle. In contrast, both PFI and PFIC topologies can guarantee no collision between CA vehicles and human-driven vehicle. Furthermore, the PFIC topology outperforms the PFI topology in terms of convergence rate of the state errors.

We further explore the platoon dynamics with all human-driven vehicles in a (linearly) unstable regime. Fig. 3 shows the platoon dynamics during the initial phase for human-driven vehicles in both stable and unstable regimes. We can observe that human-driven vehicle 6 in the unstable regime creates a larger disturbance than that in the stable regime. Moreover, human-driven vehicles with perception delay bring in small oscillations during the initially transient phase, which indicates the negative impact of perception delay on platoon stability.

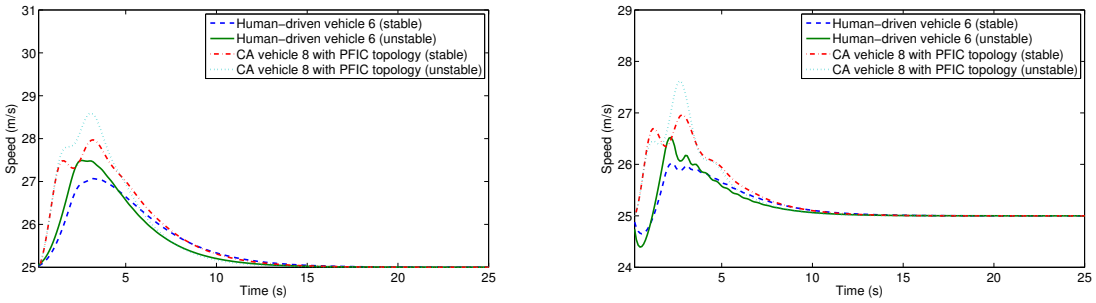

(a) Speed profile without perception delay (b) Speed profile with perception delay

Figure 3. Impact of stability of human-driven vehicles on heterogeneous platoon dynamics

5.3. *Impact of the human-driven vehicles' penetration rates*

In this part, we investigate how the penetration of the human-driven/CA vehicles affects the heterogeneous platoon dynamics. In order to neglect the impact of the vehicular order sequence on the system performance, we assume that all human-driven vehicles are deployed behind all CA vehicles in the same platoon. In this case, the AFI, PFI and PFIC have the same communication topology in the platoon control algorithms. Note that the impact of the order of vehicle types on the platoon dynamics will be studied later.

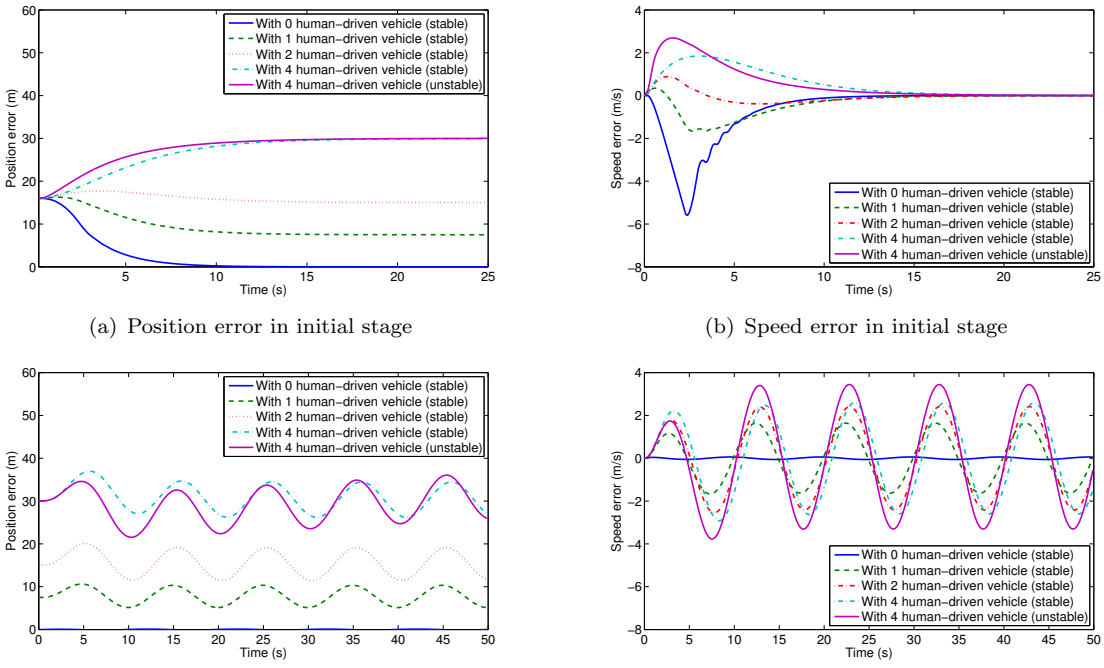

(a) Position error in initial stage (b) Speed error in initial stage

(c) Position error in perturbations (d) Speed error in perturbations

Figure 4. Heterogeneous platoon dynamics at both initial and perturbation stage with different human-driven penetrations

Let us consider four different penetration rates of the human-driven vehicles in the heterogeneous platoon (i.e. there are 0, 1, 2, and 4 human-driven vehicles), and explore the system performance in the initial phase and the continuous small perturbation situation, respectively. The simulation results are illustrated in Fig. 4. Obviously, the position errors between the leader and the last vehicle become larger with an increasing number of the human-driven vehicles in both situations. These numerical results clearly support the

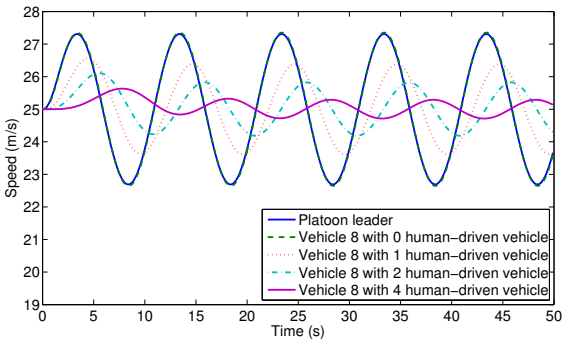

Figure 5. Speed perturbation with different human-driven penetrations

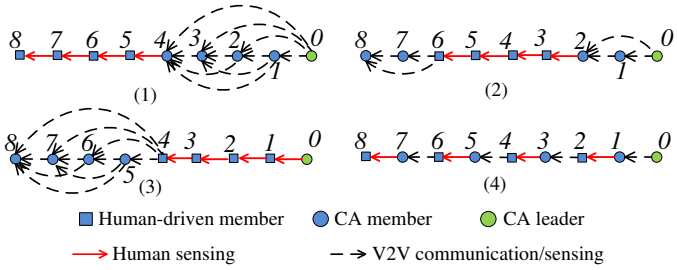

Figure 6. PFIC Communication topologies in 4 different distributions of human-driven vehicles.

conclusions in Theorem 1. Moreover, the state errors are mainly caused by the perception delay of the human-driven vehicles, compared to the impact of the communication delay of the CA vehicles. In addition, for human-driven vehicles in the unstable regime, the state errors of platoon in perturbations are larger than those for all human-driven vehicles in the stable regime, which is consistent with the findings of the platoon dynamics in the initial phase. It shall be noted that in view of the speed profile, as shown in Fig. 5, the amplitude of the speed perturbation becomes smaller with an increasing number of the human-driven vehicles. This is because, given the current model parameter settings, the equilibrium state of the human-driven vehicles is in the (linearly) stable regime.

5.4. *Impact of the order of vehicle types in the heterogeneous platoon*

To evaluate the impact of the order of the vehicle types on the platoon dynamics, let us consider four typical distributions of the human-driven vehicles in the same platoon (as shown in Fig. 6): 1) all human-driven vehicles are following all CA vehicles in the platoon as illustrated in Section 5.3, 2) all human-driven vehicles are moving in the middle of the platoon (in which both following and preceding vehicles are CA), 3) all human-driven vehicles are moving ahead of all CA vehicles and following the platoon leader, and 4) human-driven vehicles are evenly distributed in the platoon (i.e. a binary distribution).

The studied platoon contains 4 human-driven vehicles and 5 CA vehicles (including the platoon leader), with the PFIC communication topology. The state errors between the leader and the last vehicle in both initial phase and small perturbation scenarios are shown in Fig. 7. We can observe that scenario 1 outperforms all other scenarios in both situations. Specifically, scenario 1 has the fastest convergence rate during the initial phase and the minimum state errors in the small continuous perturbation case (this is because the magnitude of the perturbation is mainly decided by the perception delay). These results support our findings in Remark 3.

By contrast, other 3 scenarios show worse performance in terms of the state error convergence rate at the initial phase. The reason is that the CA vehicles behind human-

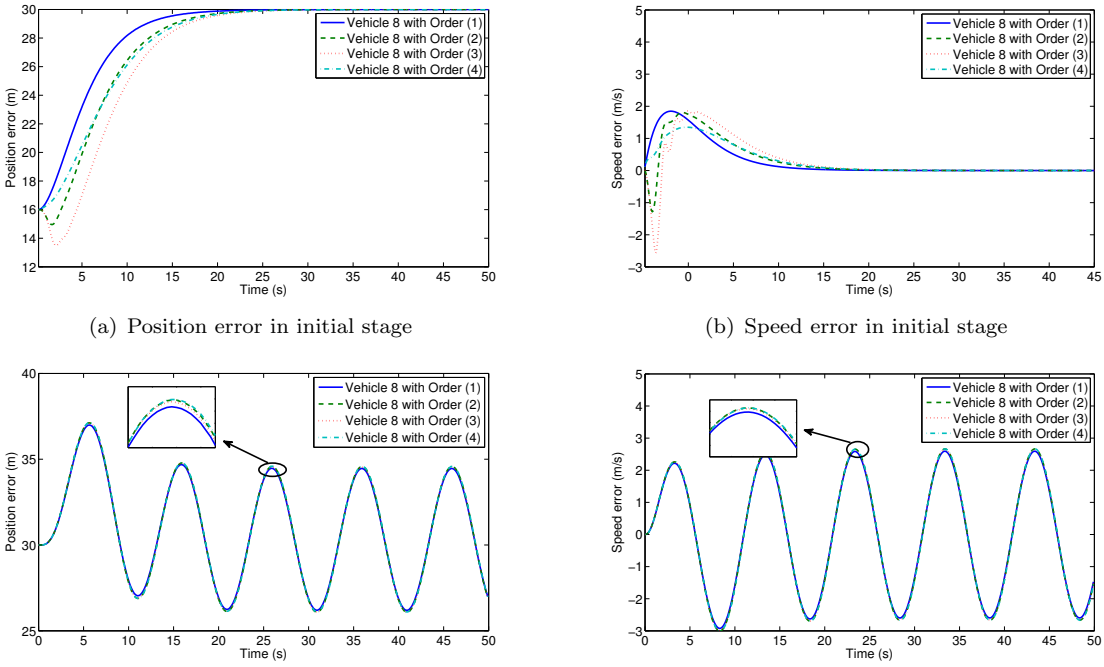

(a) Position error in initial stage

(b) Speed error in initial stage

(c) Position error in perturbations

(d) Speed error in perturbations

Figure 7. Heterogeneous platoon dynamics at both initial and perturbation stage with different human-driven penetrations

driven vehicles cannot obtain the leader's information, which consequently deteriorates the performance of the proposed control algorithm. Especially, scenario 3 has the worst performance because all human-driven vehicles move ahead of all CA vehicles. In case of a continuous small perturbations, since the leader's dynamics change slowly, the results are only slightly different amongst scenarios 2, 3, and 4. In addition, Fig. 8 illustrates the acceleration of vehicle 8 in four scenarios, which are consistent with Fig. 7.

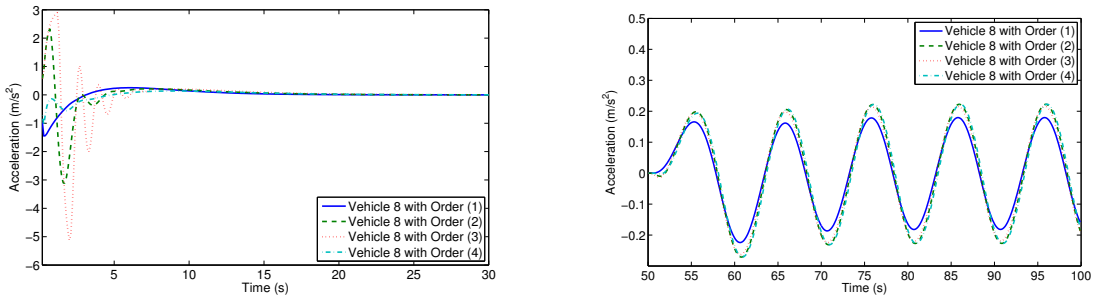

(a) Acceleration in initial stage

(b) Acceleration in perturbations

Figure 8. Heterogeneous platoon dynamics at both initial and perturbation stage with different human-driven penetrations

6. Conclusion and discussions

Although modelling the dynamics of connected and autonomous (CA) vehicles has been significantly paid attention in recent years, there is still a long way to go before a full deployment of CA vehicles on roads is viable. Therefore, a deep understanding of the dynamics of the heterogeneous traffic flow which consists of both human-driven vehicles

and CA vehicles is needed. To this end, in this paper, we have proposed a novel unified multiclass car-following model for a heterogeneous platoon moving in a single lane roadway, which theoretically explores the complex interaction between human-driven and CA vehicles. To the best of our knowledge, this is a first attempt that the complex interplay between different functional forms governing the dynamics of the human-driven and CA vehicles is explicitly demonstrated. We have then theoretically obtained the linear stability conditions of the heterogeneous platoon and characterized the transient state of the heterogeneous platoon, wherein the effects of system parameters such as human sensing delay, V2V communication delay and platoon composition structure are all taken into account. Our proposed method can be extended to capture even more complex heterogeneous traffic flow where the CA vehicles are deployed by various (linear) control algorithms. Both theoretical analysis and numerical results have indicated that the system steady-state errors are only related to the perception delay caused by the human-driven vehicles, as well as the number (penetration) of the CA/human-driven vehicles in the heterogeneous platoon. Moreover, for a given heterogeneous platoon driving with forward V2V communication topology, the optimal composition structure is that all human-driven vehicles move behind all CA vehicles.

There are a few points which are still not addressed yet in this paper. First, although we have concluded that the state errors between the leader and the members are bounded by certain value, the safety issue (i.e the collision avoidance) has not been fully addressed. Second, system uncertainties and physical limitations, for example the actuator lags, have not been considered in the vehicle dynamics, which could be modelled by a third-order system (see discussions in our previous research in Jia and Ngoduy (2016b)). Third, as aforementioned, the heterogeneous platoon can be essentially regarded as a series of adjacent sub-platoons divided by the human-driven vehicles. In this sense, the unified adjacency matrices A and B determined in Section 4.2 could be decomposed into several sub-matrices, which requires a new model description for the heterogeneous platoon. Last, the string stability for heterogeneous platoon should be further investigated. These issues are all open for the future research.

Acknowledgments

This research is partly supported by the UK Engineering and Physical Sciences Research Council (EPSRC) Career Acceleration fellowship grant EP/J002186/1 of the second author.

Appendix

Appendix A. Proof of Lemma 1

Proof. For convenience, let $H_1 \equiv \mathcal{I}^c H + f^s_{hu}(I - \mathcal{I}^c)(L + (B - D))$ and $H_2 \equiv \gamma\mathcal{I}^c H + (I - \mathcal{I}^c)(-f^{\Delta v}_{hu} L - f^v_{hu} B)$. Obviously, H_1 and H_2 are triangular matrices and their eigenvalues are the entries on the main diagonal. Moreover, the diagonal of H_1 is $\text{diag}\{..., h_{ii}, ..., f^s_{hu}, ...\}$ and the diagonal of H_2 is $\text{diag}\{..., \gamma h_{ii}, ..., -f^{\Delta v}_{hu} - f^v_{hu}, ...\}$, where $h_{ii} \geq 1$ with subscript $i \in \mathcal{I}^c$, and the position of $f^*_{hu} \in (I - \mathcal{I}^c)$. Thus both H_1 and H_2 is positive stable because $f^s_{hu} \geq 0$ while $f^{\Delta v}_{hu} \leq 0$ and $f^v_{hu} \leq 0$ so $-f^{\Delta v}_{hu} - f^v_{hu} \geq 0$.

Let λ be the eigenvalue of F, then

$$det(\lambda I_{2N} - F) = \begin{vmatrix} \lambda I_{N\times N} & -I_{N\times N} \\ H_1 & \lambda I_{N\times N} + H_2 \end{vmatrix} = det(\lambda^2 I_{N\times N} + H_2 \lambda I_{N\times N} + H_1)$$
$$= \prod_{i\in I_c} (\lambda^2 + \gamma h_{ii}\lambda + h_{ii}) \cdot \prod_{(I-I_c)} (\lambda^2 + (-f_{hu}^{\Delta v} - f_{hu}^{v})\lambda + f_{hu}^{s})$$

Obviously, every eigenvalues of F has strictly negative real part. Thus Lemma 1 holds. □

Appendix B. Proof of Theorem 1

Before the proof of Theorem 1, we first introduce the Lyapunov-Razumikhin Theorem (Hale and Lunel 1993). Let $C([-r, 0], \mathrm{R}^n)$ be a Banach space of continuous functions defined in an interval [-r,0] and taking values in R^n with a norm $\|\phi\|_c = \max_{\theta\in[-r,0]}\|\phi(\theta)\|$. Consider the following time-delay system:

$$\begin{aligned} &\dot{x} = f(t, x_t), t > 0, \\ &x(\theta) = \phi(\theta), \theta \in [-r, 0] \end{aligned} \tag{B1}$$

where $x_t(\theta) = x(t + \theta), \forall\theta \in [-r, 0]$, $f : \mathrm{R} \times C([-r, 0], \mathrm{R}^n) \to \mathrm{R}$ is a continuous function and $f(t, 0) = 0, \forall t \in \mathrm{R}$. Then we hold:

Lemma 2 (Lyapunov-Razumikhin Teheorem (Hale and Lunel 1993))**.** *Let ϕ_1, ϕ_2 and ϕ_3 be continuous, nonnegative, nondecreasing functions with $\phi_1(s) > 0$, $\phi_2(s) > 0$ and $\phi_3(s) > 0$ for $s > 0$ and $\phi_1(0) = \phi_2(0) = 0$. If there is a continuous function $V(t, x)$ such that*

$$\phi_1(\|x\|) \le V(t, x) \le \phi_2(\|x\|), t \in \mathrm{R}, x \in \mathrm{R}^n, \tag{B2}$$

In addition, there exists a continuous nondecreasing function $\phi(s)$ with $\phi(s) > s$, $s > 0$ such that the derivative of V along the solution $x(t)$ of Eq. (B1) satisfies

$$\begin{aligned} &\dot{V}(t, x) \le -\phi_3(\|x\|) \\ &if\, V(t + \theta, x(t + \theta)) < \phi(V(t, x(t))), \theta \in [-r, 0]; \end{aligned} \tag{B3}$$

then the solution $x = 0$ is uniformly asymptotically stable.

Now let's carry on the proof of Theorem 1.

Proof. Based on Lemma 1, F is Hurwitz stable. Therefore, there exists a positive definite matrix $\Phi \in \mathrm{R}^{2N\times 2N}$ such that

$$\Phi F + F^T\Phi = -I_{2N\times 2N} \tag{B4}$$

Consider Lyapunov-Razumikhin candidate function $V(\bar{\chi}) = \bar{\chi}^T\Phi\bar{\chi}$,

then

$$\dot{V}(\bar{\chi}) = \bar{\chi}^T(\Phi F + F^T\Phi)\bar{\chi} - 2\sum_{j=1}^{m}\sum_{i=0}^{m}\bar{\chi}^T\Phi\mathcal{A}_j\mathcal{A}_i\int_{-\tau_j}^{0}\bar{\chi}(t+s-\tau_j)ds$$
$$- 2\sum_{j=1}^{m}\bar{\chi}^T\Phi\mathcal{A}_k\int_{-\tau_j}^{0}\Delta(t+s)ds + 2\bar{\chi}^T\Phi\Delta$$

It is well known that for any $a, b \in \mathrm{R}^n$ and any positive-definite matrix $\Omega \in \mathrm{R}^{n\times n}$, we have: $2a^Tb \le a^T\Omega^{-1}a + b^T\Omega b$. Thus

$$\dot{V}(\bar{\chi}) \le \bar{\chi}^T(\Phi F + F^T\Phi)\bar{\chi} + \tau_j\sum_{j=1}^{m}\sum_{i=0}^{m}\bar{\chi}^T(\Phi\mathcal{A}_j^T\mathcal{A}_i^T\Phi^{-1}\mathcal{A}_i\mathcal{A}_j\Phi)\bar{\chi}$$
$$+\sum_{j=1}^{m}\sum_{i=0}^{m}\int_{-\tau_k}^{0}\bar{\chi}^T(t+s-\tau_j)\Phi\bar{\chi}(t+s-\tau_j)ds + \tau_j\sum_{j=1}^{m}\bar{\chi}^T\Phi\mathcal{A}_j\Phi^{-1}\mathcal{A}_j^T\Phi^T\bar{\chi}$$
$$+\sum_{j=1}^{m}\int_{-\tau_j}^{0}\Delta^T(t+s)\Phi\Delta(t+s)ds + 2\bar{\chi}^T\Phi\Delta$$

Choose $\phi_s = \zeta s$ with the constant $\zeta > 1$, in case of $V(\bar{\chi}(t+s-\tau_j)) = \bar{\chi}^T(t+s-\tau_j)\Phi\bar{\chi}(t+s-\tau_j) \le \zeta V(\bar{\chi}), \tau_j \le \tau$, we then have

$$\dot{V}(\bar{\chi}) \le -\bar{\chi}^T\left\{I - \tau\left[\sum_{j=1}^{m}\sum_{i=0}^{m}(\Phi\mathcal{A}_j^T\mathcal{A}_i^T\Phi^{-1}\mathcal{A}_i\mathcal{A}_j\Phi + \zeta\Phi) + \sum_{j=1}^{m}\Phi\mathcal{A}_j\Phi^{-1}\mathcal{A}_j^T\Phi^T\right]\right\}\bar{\chi}$$
$$+\sum_{j=1}^{m}\int_{-\tau_j}^{0}\Delta^T(t+s)\Phi\Delta(t+s)ds + 2\bar{\chi}^T\Phi\Delta$$

We denote $\psi := \max\sum_{j=1}^{m}\sum_{i=0}^{m}(\|\Phi\mathcal{A}_j^T\mathcal{A}_i^T\Phi^{-1}\mathcal{A}_i\mathcal{A}_j\Phi\| + \|\zeta\Phi\|) + \sum_{j=1}^{m}(\|\Phi\mathcal{A}_j\Phi^{-1}\mathcal{A}_j^T\Phi^T\|)$.

Obviously, for $V(\bar{\chi}) = \bar{\chi}^T\Phi\bar{\chi}$, we have

$$\underline{\lambda}\|\bar{\chi}\|^2 \le V(\bar{\chi}) \le \bar{\lambda}\|\bar{\chi}\|^2$$

where $\underline{\lambda}$ and $\bar{\lambda}$ are the minimum and maximum of the eigenvalues of Φ, which means

$$\|\bar{\chi}\| \le \frac{1}{\sqrt{\underline{\lambda}}}\sqrt{V(\bar{\chi})}$$

On the other hand,

$$\min\frac{\bar{\chi}^T\bar{\chi}}{\bar{\chi}^T(\Phi)\bar{\chi}} \ge \frac{1}{\bar{\lambda}} = 2\kappa$$

where $\kappa = \frac{1}{2\bar{\lambda}} > 0$. Then if $\tau \leq \frac{1}{2\psi}$, we have

$$\dot{V}(\bar{\chi}) \leq -(\frac{1}{2}-\tau\psi)\bar{\chi}^T\bar{\chi}-\kappa V(\bar{\chi})+|\bar{\delta}|^2\bar{\lambda}\sum_{j=1}^{m}\tau_j+2\sqrt{\frac{|\bar{\delta}|^2\bar{\lambda}^2}{\kappa\underline{\lambda}}\kappa V(\bar{\chi})} \leq -\kappa(1-2\psi\tau)V(\bar{\chi})+|\bar{\delta}|^2(\bar{\lambda}\sum_{j=1}^{m}\tau_j+\frac{\bar{\lambda}^2}{\kappa\underline{\lambda}})$$

Let $\eta := \kappa(1-2\psi\tau)$, then we have

$$V(\bar{\chi}) \leq V(\bar{\chi}(0))e^{-\eta t} + \frac{C_0}{\eta}(1-e^{-\eta t}) \tag{B5}$$

where $C_0 \equiv |\bar{\delta}|^2(\frac{\bar{\lambda}^2}{\kappa\underline{\lambda}} + \bar{\lambda}\sum_{j=1}^{m}\tau_j)$.

Therefore, we can conclude the system will attain the bounded state error at an exponentially converging speed η.

This completes the proof of Theorem.

□

References

Bando, M., Hasebe, K., Nakayama, A., Shibata, A., Sugiyama, Y., 1995. Dynamical Model of Traffic Congestion and Numerical Simulation. Physical Review E 51, 1035–1042.

Bansal, P., Kockelman, K. M., 2017. Forecasting Americans' long-term adoption of connected and autonomous vehicle technologies. Transportation Research Part A: Policy and Practice 95, 49–63.

Bernardo, M., Salvi, A., Santini, S., 2015. Distributed consensus strategy for platooning of vehicles in the presence of time-varying heterogeneous communication delays. IEEE Transactions on Intelligent Transportation Systems 16 (1), 102–112.

Delis, A. I., Nikolos, I. K., Papageorgiou, M., 2015. Macroscopic traffic flow modeling with adaptive cruise control: Development and numerical solution. Computers and Mathematics with Applications 70, 1921–1947.

Dey, K. C., Yan, L., Wang, X., Wang, Y., Shen, H., Chowdhury, M., Yu, L., Qiu, C., Soundararaj, V., 2016. A Review of Communication, Driver Characteristics, and Controls Aspects of Cooperative Adaptive Cruise Control (CACC). IEEE Transactions on Intelligent Transportation Systems 17 (2), 491–509.

Dunbar, W.and Caveney, D., 2012. Distributed Receding Horizon Control of Vehicle Platoons: Stability and String Stability. Automatic Control, IEEE Transactions on 57, 620–633.

Fernandes, P., 2012. Platooning with ivc-enabled autonomous vehicles: Strategies to mitigate communication delays, improve safety and traffic flow. IEEE Transactions on Intelligent Transportation Systems 13, 91–106.

Ge, J. I., Orosz, G., 2014. Dynamics of connected vehicle systems with delayed acceleration feedback. Transportation Research Part C: Emerging Technologies 46, 46–64.

Ghasemi, A., Kazemi, R., Azadi, S., 2013. Stable decentralized control of a platoon of vehicles with heterogeneous information feedback. IEEE Transactions on Vehicular Technology 62 (9), 4299–4308.

Gong, S., Shen, J., Du, L., 2016. Constrained optimization and distributed computation based car following control of a connected and autonomous vehicle platoon. Transportation Research Part B: Methodological 94, 314–334.

Guo, G., Yue, W., 2011. Hierarchical platoon control with heterogeneous information feedback. IET Control Theory & Applications 5 (15), 1766–1781.

Hale, J. K., Lunel, S. M. V., 1993. Introduction to Functional Differential Equations. Springer-Verlag.

Jia, D., Lu, K., Wang, J., Zhang, X., Shen, X., 2016. A survey on platoon-based vehicular cyber-physical systems. IEEE Communications Surveys & Tutorials 18 (1), 263–284.

Jia, D., Ngoduy, D., 2016a. Enhanced cooperative car-following traffic model with the combination of V2V and V2I communication. Transportation Research Part B 90, 172–191.

Jia, D., Ngoduy, D., 2016b. Platoon based Cooperative Driving Model with Consideration of Realistic Inter-vehicle Communication. Transportation Research Part C 68, 245–264.

Jiang, R., Wu, Q., Zhu, Z., 2001. Full velocity difference model for a car-following theory. Physical Review E 64, 017101–017104.

Kesting, A., 2007. Microscopic modeling of human and automated driving: Towards traffic-adaptive cruise control. Ph.D. dissertation.

Kesting, A., Treiber, M., Helbing, D., 2010a. Enhanced Intelligent Driver Model to Access the Impact of Driving Strategies on Traffic Capacity . Philosophical Transactions of the Royal Society A 368, 4585–4605.

Kesting, A., Treiber, M., Schonhof, M., Helbing, D., 2008. Adaptive cruise control design for active congestion avoidance. Transportation Research Part C 16 (6), 668–683.

Kim, Y., Peeta, S., He, X., 2016. An analytical model to characterize the spatiotemporal propagation of information under vehicle-to-vehicle communications. IEEE Transactions on Intelligent Transportation Systems in press.

Lestas, I., Vinnicombe, G., 2007. Scalability in heterogeneous vehicle platoons. Proceedings of the American Control Conference, 4678–4683.

Levin, M. W., Boyles, S. D., 2016. A multiclass cell transmission model for shared human and autonomous vehicle roads. Transportation Research Part C: Emerging Technologies 62, 103–116.

Ling, X., Gao, F., 2011. Practical string stability of platoon of adaptive cruise control vehicles. IEEE Transactions on Intelligent Transportation Systems 12 (4), 1184–1194.

Liu, B., Jia, D., Lu, K., Ngoduy, D., Wang, J., Wu, L., 2017. A joint control-communication design for reliable vehicle platooning in hybrid traffic. IEEE Transactions on Vehicular Technology 66 (10), 9394–9409.

Middleton, R., Braslavsky, J., 2012. String instability in classes of linear time invariant formation control with limited communication range. IEEE Transactions on Automatic Control 55 (7), 1519–1530.

Monteil, J., Billot, R., Sau, J., El Faouzi, N.-E., 2014. Linear and weakly nonlinear stability analyses of cooperative car-following models. IEEE Transactions on Intelligent Transportation Systems 15, 2001–2013.

Naus, G. J. L., Vugts, R. P. A., Ploeg, J., van de Molengraft, M. R. J. G., Steinbuch, M., 2010. String-stable cacc design and experimental validation: A frequency-domain approach. IEEE Transactions on Vehicular Technology 59 (9), 4268–4279.

Ngoduy, D., 2013a. Platoon-based macroscopic model for intelligent traffic flow. Transportmetrica B 1, 153–169.

Ngoduy, D., 2013b. Analytical studies on the instabilities of heterogeneous intelligent traffic flow. Communications in Nonlinear Science and Numerical Simulation 18 (10), 2699–2706.

Ngoduy, D., 2013c. Instability of cooperative adaptive cruise control traffic flow: a macroscopic approach. Communications in Nonlinear Science and Numerical Simulation 18 (10), 2838–2851.

Ngoduy, D., 2015a. Effect of the car-following combinations on the instability of heterogeneous traffic flow. Transportmetrica B: Transport Dynamics 3 (1), 44–58.

Ngoduy, D., 2015b. Linear stability of a generalized multi-anticipative car following model with time delays. Communications in Nonlinear Science and Numerical Simulation 22, 420–426.

Ngoduy, D., Jia, D., 2017. Multi anticipative bidirectional macroscopic traffic model considering cooperative driving strategy. Transportmetrica B 5, 100–114.

Ngoduy, D., Tampere, C., 2009. Macroscopic effects of reaction time on traffic flow characteristics. Physica Scripta 80, 025802.

Nikolos, I. K., Delis, A. I., Papageorgiou, M., 2015. Macroscopic modelling and simulation of acc and cacc traffic. IEEE Conference on Intelligent Transportation Systems (7313436), 2129–2134.

Öncü, S., Ploeg, J., van de Wouw, N., Nijmeijer, H., 2014. Cooperative Adaptive Cruise Control : Network-Aware Analysis of String Stability. IEEE Transactions on Intelligent Transportation Systems 15 (4), 1527–1537.

Qu, Z. Q. Z., Wang, J. W. J., Hull, R., 2008. Cooperative Control of Dynamical Systems With Application to Autonomous Vehicles. IEEE Transactions on Automatic Control 53 (4), 894–911.

Saifuzzaman, M., Zheng, Z., 2014. Incorporating human-factors in car-following models: a review of recent developments and research needs. Transportation Research Part C 48, 379–403.

Saifuzzaman, M., Zheng, Z., Haque, M. M., Washington, S., 2015. Revisiting the taskcapability interface model for incorporating human factors into car-following models. Transportation Research Part B 82, 1–19.

Sau, J., Monteil, J., Bouroche, M., 2017. State-space linear stability analysis of platoons of cooperative vehicles. Transportmetrica B: Transport Dynamics "in press", 1–26.

Segata, M., Joerer, S., Bloessl, B., Sommer, C., Dressler, F., Cigno, R. L., 2014. Plexe: A platooning extension for veins. In: Proceedings of 6th IEEE Vehicular Networking Conference. Paderborn, Germany, pp. 53–60.

Seiler, P., Pant, A., Hedrick, K., 2004. Disturbance propagation in vehicle strings. Automatic Control, IEEE Transactions on 49 (10), 1835–1841.

Shaw, E., Hedrick, J. K., 2007. String stability analysis for heterogeneous vehicle strings. In: Proceedings of the American Control Conference. pp. 3118–3125.

Talebpour, A., Mahmassani, H. S., 2016. Influence of connected and autonomous vehicles on traffic flow stability and throughput. Transportation Research Part C 71, 143–163.

Tang, T. Q., Shi, W. F., Shang, H. Y., 2014. An extended car-following model with consideration of the reliability of inter-vehicle communication. Measurement 58, 286–293.

Treiber, M., Kesting, A., Helbing, D., 2006. Delays, inaccuracies and anticipation in microscopic traffic model. Physica A 360, 71–88.

van Arem, B., van Driel, C. J. G., Visser, R., 2006. The impact of cooperative adaptive cruise control on traffic-flow characteristics. IEEE Transactions on Intelligent Transportation Systems 7 (4), 429–436.

Wang, L. Y., Syed, A., Yin, G., Pandya, A., Zhang, H., 2014. Coordinated vehicle platoon control : Weighted and constrained consensus and communication network topologies. Journal of Systems Science and Complexity 27 (4), 605–631.

Wang, M., Hoogendoorn, S. P., Daamen, W., van Arem, B., Shyrokau, B., Happee, R., 2016. Delay-compensating strategy to enhance string stability of adaptive cruise controlled vehicles. Transportmetrica B: Transport Dynamics "in press", 1–19.

Xu, L., Wang, L. Y., Yin, G., Zhang, H., 2014. Communication information structures and contents for enhanced safety of highway vehicle platoons. IEEE Transactions on Vehicular Technology 63 (9), 4206–4220.

Zheng, Y., Eben Li, S., Wang, J., Cao, D., Li, K., 2016. Stability and Scalability of Homogeneous Vehicular Platoon: Study on the Influence of Information Flow Topologies. IEEE Transactions on Intelligent Transportation Systems 17 (1), 14–26.

Zheng, Z., 2014. Recent developments and research needs in modeling lane changing. Transportation Research Part B 60, 16–32.